Biotechnology Reports 17 (2018) 137–147

Contents lists available at ScienceDirect

Biotechnology Reports

journal homepage: www.elsevier.com/locate/btre

Full Length Article

Evaluation of the ethanol tolerance for wild and mutant *Synechocystis* strains by flow cytometry

Teresa Lopes da Silva[a,*], Paula C. Passarinho[a], Ricardo Galriça[a], Afonso Zenóglio[a], Patricia Armshaw[b], J. Tony Pembroke[b], Con Sheahan[c], Alberto Reis[a], Francisco Gírio[a]

[a] Laboratório Nacional de Energia e Geologia, I.P., Unidade de Bioenergia, Estrada do Paço do Lumiar 22, 1649-038, Lisbon, Portugal
[b] Bernal Institute, Department of Chemical Sciences, School of Natural Sciences University of Limerick, Ireland
[c] School of Engineering, University of Limerick, Ireland

ARTICLE INFO

Article history:
Received 2 November 2017
Received in revised form 31 January 2018
Accepted 13 February 2018
Available online 15 February 2018

Keywords:
Synechocystis wild and mutant strains
Ethanol
Tolerance
Membrane permeability
Enzymatic activity
Flow cytometry

ABSTRACT

Flow cytometry was used to evaluate the effect of initial ethanol concentrations on cyanobacterial strains of *Synechocystis* PCC 6803 [wild-type (WT), and ethanol producing recombinants (UL 004 and UL 030)] in batch cultures. Ethanol recombinants, containing one or two metabolically engineered cassettes, were designed towards the development of an economically competitive process for the direct production of bioethanol from microalgae through an exclusive autotrophic route.

It can be concluded that the recombinant *Synechocystis* UL 030 containing two copies of the genes per genome was the most tolerant to ethanol. Nevertheless, to implement a production process using recombinant strains, the bioethanol produced will be required to be continuously extracted from the culture media via a membrane-based technological process for example to prevent detrimental effects on the biomass. The results presented here are of significance in defining the maximum threshold for bulk ethanol concentration in production media.

1. Introduction

The global energy crisis and the international political pressure to reduce greenhouse gases (GHG) have driven the search for renewable energy alternatives to replace traditional energy sources [1]. The production of bioethanol has received increasing attention recently, as it is one major type of biofuel that can be blended with gasoline for use in current internal combustion engines powertrains.

Currently, most bioethanol is obtained by fermentation of starch-based cereals and sugarcane. However, biofuels produced from food crops are in competition with the food and animal feed industries, increasing food prices and rising strong opposition in the EU and globally [2]. On the other hand, forest and agricultural lignocellulosic residual materials display a severe recalcitrance towards fractionation for sugars production, and the inability of microorganisms to efficiently ferment lignocellulosic hydrolysates still reduce the bioethanol process yield from these plentiful materials [3].

Therefore, new (bio)technical routes for the production of bioethanol that are not lignocellulosic biomass based but directly photosynthesis-derived are the subject of intense research [4–6]. Cyanobacteria are prokaryotes which exhibit diversity in metabolism, structure, morphology and habitat and perform photosynthesis similar to that performed by higher plants [7]. In addition, as cyanobacteria have simple growth requirements, grow to high densities, and use light, carbon dioxide, and other inorganic nutrients efficiently, they could be attractive hosts for production of valuable organic products [8].

Synechocystis sp. strain PCC 6803 (hereafter *Synechocystis*) is a model cyanobacterium for genetic manipulation and has been already widely used as a cell factory to produce a range of biotechnological products such as ethanol, fatty acids, biopolymers and sugars [6]. Within the FP7 DEMA project (Direct Ethanol from MicroAlgae) the utility of this model cyanobacterium to produce ethanol at a low cost was investigated (http://www.dema-etoh.eu/en/). A non-native ethanol biosynthesis pathway has been integrated into *Synechocystis* and a library of ethanol-producing recombinants has been generated and characterized, both genetically and phenotypically, including strains UL 004 (a single copy strain) and UL 030 (a double copy strain), which, under laboratory conditions, have been producing encouraging levels of ethanol [9].

* Corresponding author.
E-mail address: teresa.lopessilva@lneg.pt (T. Lopes da Silva).

https://doi.org/10.1016/j.btre.2018.02.005

Cyanobacteria and the model organism *Synechocystis* are known to be sensitive to ethanol [10], which may limit efforts to increase ethanol production levels in these microorganisms thus examination of production levels and tolerance are key determinants of the utility of such a cell factory.

Flow cytometry has been extensively used in microalgae stress studies, being considered an useful technique to detect microalgal cell stress response to environmental stress [11–16].

The detection of cellular esterase activity (which concerns common enzymes in viable cells of both plants and animals) by cytometry, can be an indicator of the cell viability as well as of metabolic activity [16]. In addition, it is an effective bioassay since it can offer acute and sub-lethal endpoints and help to identify inhibition mechanisms [12,14,15].

Ethanol toxicity, on the other hand, is generally attributed to the preferential partition of ethanol in the hydrophobic environment of microbial membrane lipid bilayers, resulting in the perturbations of the membrane structure. Therefore, as the plasma membrane protects the cell from its external environment, membrane integrity is considered an important cell viability indicator when studying the effect of solvents such as ethanol on microbial cells [17].

Franklin et al. [12] developed a rapid enzyme inhibition detection method based on Fluorescein diacetate/Propidium iodide (FDA/PI) staining for microalgae using flow cytometry, which was successfully utilized by Xi et al. [14] to evaluate the viability of the cyanobacterium *Microcystis aeruginosa*.

To understand the mechanism(s) of ethanol tolerance in *Synechocystis* and two recombinants with improved ethanol production capacity (UL 004 and UL 030, engineered at the University of Limerick), the present work evaluated their stress response when grown in batch cultivation in the presence of increasing initial ethanol concentrations. Flow cytometry was then used to monitor the cellular enzymatic activity and membrane integrity during the growth assays.

The results reported increase our understanding of ethanol tolerance of *Synechocystis* cells (wild-type and recombinant strains), which may allow construction of more robust ethanol producers cyanobacterial strains.

2. Materials and methods

2.1. Synechocystis *strains*

Synechocystis (kindly provided Prof. Klaas Hellingwerf, University of Amsterdam) was routinely maintained at 30 °C on BG-11 media supplemented with 10 mM TES-NaOH (pH 8.2), 20 mM glucose and 0.3% (w/v) sodium thiosulfate. *Synechocystis* UL 004 is an ethanol producing strain of PCC 6803 containing a single gene cassette which consists of the P_{psbAII} light inducible promoter from *Synechocystis* [18], the pyruvate decarboxylase, *pdc*, gene from *Zymomonas mobilis* (Zm*pdc*), the native *Synechocystis adhA* gene [19], and the kanamycin resistance gene from ICE R391 [20]. The construct also contains 500 bp at each end with homology to the PSBAII neutral site to allow homologous recombination into this neutral site [21]. For construction of UL 004 (Fig. 1) the single cassette strain, a biobrick cloning and construction approach was used [22,23]. The kanamycin and *adhA* genes were amplified from their respective genomes with primers as described (primers 1 to 4, Table 1) to allow a subsequent overlap PCR to link the kanamycin and *adhA* genes. pMOTA [5] was linearised and used as the source or the Zm*pdc* fused to the P_{psbAII} promoter and the 500 bp homologous regions to allow integration into the PSBA2 neutral site. Homologous recombination via the In-Fusion® HD cloning kit (Clontech Laboratories Inc. 2014, Takara Bio Company, Mountain view, California, USA) was used to recombine the overlaping PCR product [KanR/*adhA* and linearised pMOTA], this was cloned into pUC18 [24] again via In-Fusion® HD cloning resulting in the construction of the UL 004 plasmid. Verification of the UL 004 plasmid was carried out via PCR amplification of the construct (primers 15 and 66, Table 1) followed by sequencing. The *Synechocystis* homologous psbA2 site within the UL 004 plasmid was utilized to allow homologous integration of the UL 004 cassette into the psbA2 neutral site in *Synechocystis* [21]. Transformants of wild type *Synechocystis* [25] were sub-cultured in BG-11 media containing increasing concentrations of kanamycin [5–50 μg/ml] until full integration of the UL 004 cassette was verified. Verification of integration into the psbA2 neutral site was carried out with appropriate primers (primer 5 and primer 6, Table 1) that bound the flanking homologous insertion site within psbA2. Wild type *Synechocystis* amplified with these primers generated a PCR product approximately 1.2 kb in size, insertion of the UL 004 cassette resulted in the amplification of a ~4 kb PCR product. Strains, designated UL 004, were also assayed for ethanol production to determine functionality of the cassette.

A double cassette strain, UL 030, was then constructed in a similar manner to that reported by Gao et al. [4] (Fig. 1) by inserting a second cassette into UL 004. This second cassette was inserted into the *phaAB* genes, eliminating PHA accumulation and storage, and hence, facilitating more pyruvate availability for conversion to ethanol [4]. Initially the UL004 plasmid was modified to remove the kanamycin resistance determinant and replace it with zeocin resistance utilising similar homologous recombination techniques as described above and primers as per Table 1. The UL 004 plasmid was linearised with inverse PCR at regions flanking the kanamycin resistance gene, thereby linearising the plasmid while removing the kanamycin gene. The zeocin resistance gene was amplified from pcDNA3.1 (Invitrogen, ThermoFischer Scientific) with primers 9 and 10 (Table 1). Homologous recombination of the linearised UL 004 plasmid lacking the kanamycin determinant and amplified zeocin resistance gene resulted in the generation of UL004-zeocin, a zeocin resistance version of the UL 004 plasmid.

Similarly a second unique plasmid was generated containing the *phaAB* genes and flanking regions from *Synechocystis*. The

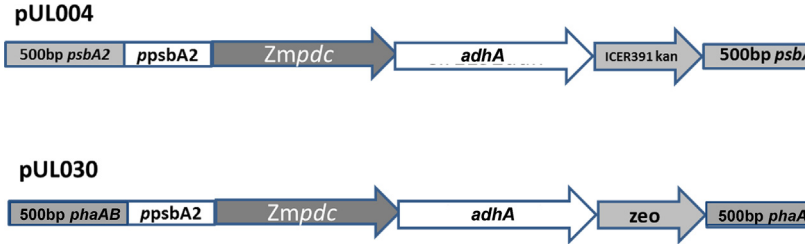

Fig. 1. Construction of UL 004 (a single cassette strain) and UL 030 (a double cassette strain).
The Genbank assession of the *Synechocystis adhA* was Gen Bank: AP012205.1 (nt 3,530,233 to 3,531,243), CDS: BAK51882.1; The GeneBank assession of the *Zymomonas pdc* was Gene Bank HM235920.1 (nt 493.2199) CDS: ADK13058.1.

Table 1
Primers used to construct the recombinant metabolically engineered ethanol cassettes UL 004 and UL 030. Primer sequences are shown in the 5′ to 3′ direction and were supplied by Eurofins Genomics.

Primer	Sequence	Description
1	TATCAATTCGAGCTCGGTACCCAAACTAGTATGTAGGGTGAGGTTATAGCTATGATTAAAGCCTACGCTGCCCTGG	Forward primer for slr1192 with targeted insertion site for pMota
2	TTGTGCAATATAACATGGGTAATCCTTTGCCTCGGCTATCTGTCA	Reverse primer for slr1192 with homology for overlap to Kan^R
3	AGATAGCCGAGGCAAAGGATTACCCATGTTATATTGCACAAGATAA	Forward primer for Kan^R with overlap to slr1192.
4	CAATTTGCAGATTATTCAGTTGGCATTACACCAAGGAATTAGGATCCTAGTACCGTCCGGATACTGCCAGAT	Reverse primer for Kan^R with targeted insertion site for pMOTA
5	GTCAGTTCCAATCTGAACATCGA	Verification Primer UL004
6	CAATTTGCAGATTATTCAGTTGGCAT	Verification Primer UL004
7	GTCCTTTTTGTTAACGTTGCC	Verification Primer UL030
8	GGCTTTTTTGTCGTCCC	Verification Primer UL030
9	GCTAGGCAAAACCCCTGACAGATAGCCGAGGCAAAGGATTGCTATTCCAGAAGTAGTGAGGA	Forward primer for amplification of zeocin resistance from pcDNA3.1 with homology to insertion site in UL004 plasmid
10	CAGATTATTCAGTTGGCATTACACCAAGGAATTAGGATCCGCTATGACCATGATTACGCCAA	Reverse primer for amplification of zeocin resistance from pcDNA3.1 with homology to insertion site in UL004 plasmid
11	ATACTGCAGGTCCTTTTTGTTAACGTTGCC	Forward primer to amplify phbAB region
12	ATAGGATCCGGCTTTTTTGTCGTCCC	Reverse primer to amplify phbAB region
13	GGGAGGAGAAAATTAGGATTCTTGCACAGTACCGCAAAAGCATGGAAAAAACGACAATTACAAG	Forward Primer to amplify UL004-zeocin with relevant homology to pUC18-PHB
14	TGCCAAATTAATCCCCATAATTGAGCTGGAGGCGGAGTTAGCTATGACCATGATTACGCCAAG	Reverse Primer to amplify UL004-zeocin with relevant homology to pUC18-PHB
15	ACTTCTCGAGCTCTGTACATGTCCG	UL004 forward primer to amplify from pUL004
16	TAGCCCGTTGAATCTCACAC	UL004 reverse primer to amplify from pUL004

*pha**AB* genes were amplified with primers 11 and 12 (Table 1) and the resultant PCR amplicon and pUC18 plasmid [24] were digested with PstI and BamHI and ligated together to generate pUC18-PHB. Finally the relevant ethanol producing region from UL004-zeocin [PpsbAII promotoer, Zm*pdc*, *adhA*, zeocin resistant determinant] were amplified with primers 13 and 14 below. pUC18-PHB was linerised with primers that removed the *pha*AB genes while preserving the flanking regions. Homologous recombination as described above was utilized to replace the *pha*AB genes with the UL004-zeocin amplicion resulting in a plasmid that contained homology to the regions flanking the *pha*AB genes and a zeocin resistant ethanol producing construct termed UL 030 (Fig. 1). pUL030 was transformed into UL 004 (already carrying a single cassette) [25] to generate a double cassette strain (Fig. 1), designated UL 030. The presence of the second cassette was selected via growth on increasing concentrations of zeocin (5–100 μg/ml) and stable transformants were verified using PCR amplification (primers 7 and 8, Table 1) followed by sequencing the amplicon and monitoring ethanol productivity.

2.2. Inoculum

Seed cultures of the strains were prepared by adding 500 ml of fresh BG-11 medium to small volumes of late exponential cultures in 1 l shake flasks, and kept at room temperature under orbital motion (100 rpm) and fluorescent light for five days. Kanamycin sulfate (50 mg/l) and kanamycin sulfate (50 mg/l) plus zeocin (5 mg/l) were added respectively to UL 004 and UL 030 cultures.

Prior to inoculation, the exponentially growing cells were concentrated by centrifugation (7 min; 10 000 rpm) and washed with fresh medium without antibiotics.

2.3. Cyanobacteria cultures

Cultures of *Synechocystis* wild (WT) and recombinant strains UL 004 and UL 030 were developed in 500 ml Erlenmeyer flasks containing 100 ml of standard BG-11 media supplemented with ethanol at initial concentrations of 1, 5, 10, 15, 20, 30 and 40 g/l, and inoculated with 1 ml of a cell concentrated suspension (initial biomass concentration of 30 mg dry biomass/l). For each strain, a control experiment was conducted, under the same conditions, but without ethanol. In addition, for each ethanol concentration, growth trials were performed in duplicate and in parallel with a blank test without cyanobacterial cells, to evaluate ethanol evaporation throughout the experiment.

The inoculated flasks were capped with cotton wool and kept at 30 °C in an incubator, under orbital shaking (135 rpm) and a photosynthetic photon flux density (PPFD) of 24 μE/(m^2s). The cultures were at-line monitored in terms of biomass concentration by OD readings at 730 nm, after sample sonication, using a spectrophotometer Hitachi U-2000, until the stationary phase was reached and the readings did not change significantly for 4 or 5 days. In the same way, the enzymatic activity and membrane integrity were monitored (by flow cytometry, Section 2.4) as well as morphology (fluorescence microscope, Section 2.6). The ethanol level was determined by gas chromatography after sample centrifugation at 15 000 rpm for 5 min (Section 2.7). Biomass concentration values were obtained building a correlation between OD_{730} readings of sonicated samples and the dry biomass weight (at 80 °C for 18 h).

2.4. Flow cytometry

Flow cytometry (FC) was performed in a device (FACSCalibur, Becton Dickinson) containing an argon laser and a red diode laser, emitting at 488 and 635 nm respectively, and four photomultipliers: FL1 (green; 530 ± 30 nm), FL2 (Yellow; 585 ± 42 nm), FL3 (Red; 670 nm) and FL4 (Orange; 661 ± 16 nm).

FC analysis was performed at regular intervals to assay cell status in terms of enzymatic activity, using the stain carboxyfluorescein diacetate (CFDA) and the method described by Franklin et al. [12] with modifications. As compared with fluorescein (FDA), carboxyfluorescein contains extra negative charges and is therefore better retained in cells. CFDA is a cell-permeant molecule which diffuses in all cells. Once within active cells, the CFDA substrate is cleaved by non-specific esterases, releasing a polar fluorescein product that is retained inside cells with intact membranes. In this situation, under blue light

excitation, the cells fluoresce green, being detected in the FL1 channel. Retention of the dye inside the cell indicates functional cytoplasmic enzymes and membrane integrity, while injured or dead cells do not stain because they lack enzyme activity and CFDA diffuses freely through damaged membranes [17]. To determine whether reduction of CFDA fluorescence is due to membrane disruption (i.e. reduced uptake of the dye) or inhibition of intracellular esterases, cells were also stained with the nucleic acid stain, propidium iodide (PI) [14]. Propidium iodide only enters cells with damaged membranes and stains nucleic acids; thus, PI can discriminate between live viable and nonviable (i.e. fluorescent) cells. PI is excited at 488 nm and emits at a maximum wavelength of 617 nm, being detected in the FL2 or FL3 channels.

Before running in the flow cytometer, samples were sonicated for 10 s to prevent aggregate formation and subsequent clogging of the laminar flow chamber.

Samples were diluted adjusting the dilution factor to ensure a suitable number of events, between 800 and 1000 per second. For membrane enzymatic activity detection, samples were diluted in phosphate citrate (McIlvaine buffer, pH 4) buffer (final volume of 500 μl), stained with 4 μl of a CFDA stock solution (with a concentration of 10 mg/ml), incubated in the darkness for 40 min, and then analyzed.

For membrane integrity detection, samples were diluted in phosphate saline buffer (PBS, pH 7.3). Samples with a final volume of 500 μl were stained with 5 μl of a PI stock solution (with a concentration of 1 mg/ml) and analyzed immediately.

Forward scatter (FSC), side scatter (SSC) and fluorescence signals were plotted in a logarithmic scale and data were analyzed with Cellquest software. Average FSC, SSC and fluorescence signals, and cell population percentages were calculated using the free data analysis Flowing Software. Sample autofluorescence was also determined to establish a baseline control regarding the stained samples analysis. The cyanobacteria cells populations were discriminated based on the forward scatter (FSC) *versus* chlorophyll fluorescence (FL3) plot.

2.5. Fungal contamination detection

To ensure that *Synechocystis* (WT and UL 004 strains) filamentous aggregates observed at higher ethanol concentrations (30 g/l and 40 g/l) were not fungal contaminations, UL004 strain was grown in the presence of 30 g/l ethanol and kanamycin.

After 400 h, samples were withdrawn and observed under the fluorescent microscope, using a blue filter, to detect chlorophyll pigment. Samples were also plated in Rose Bengal medium. Afterwards, the medium was centrifuged and the pellet was re-inoculated into fresh medium with kanamycin but without ethanol.

2.6. Synechocystis *cells morphology*

Cells from cultures at different ethanol concentrations were observed under an optical microscope Olympus BX60 (Tokyo, Japan) to detect morphological changes.

2.7. Gas chromatography

To assess ethanol concentration, the samples were analyzed in a HP 5890 device equipped with a flame ionization detector, on-column injector and a 2 m and 1/8'' diameter column (4% Carbowax 20 M, 1% trimesilic acid, 80-20 Carbopack BDA). The injector, detector and oven temperatures were respectively 150, 200 and 110 °C. Helium was used as carrier gas and isopropanol as an internal standard.

3. Results and discussion

Recent efforts have been made to elucidate the mechanisms underlying the resistance of *Synechocystis* to ethanol [19,26–30]. Wang et al. (2012) [26] applied a quantitative RNA-Seq based transcriptomics approach combined with quantitative reverse-transcript PCR (RT-PCR) analysis to reveal the global transcriptomic responses to ethanol in *Synechocystis* and stated that the cyanobateria probably employed multiple and synergistic resistance mechanisms in dealing with ethanol stress. Song et al. (2014) [27] revealed that the Sll0794 transcriptional regulator is related directly to ethanol tolerance in *Synechocystis*. Zhang et al. [28] stated that slr0982 is involved in ethanol tolerance in *Synechocystis*. Zhu et al. [29] using targeted LC–MS and untargeted GC–MS approaches found that the genes *sll1392*, *sll1712* and *slr1860* may be involved in the regulation of ethanol tolerance. According to Vidal et al. [30], the lack of the protein *adhA* in the wild-type strain reduces survival to externally added ethanol at lethal concentration of 4% (v/v).

Other approaches can be used to complement these studies, such as flow cytometry, which allows cellular changes detection in terms of cell functions or compartments to environmental stress [11–16] which was used in the present work to study the ethanol effect on *Synechocystis* strains, as described in the following sections.

3.1. Preliminary flow cytometric controls

To demonstrate the possibility of using flow cytometry to monitor WT, UL 004 and UL 030 cell status and morphological changes during the experiments with ethanol, it was essential to carry out several preliminary controls, using exponential growing cells and ethanol-treated cells. These were then used for further comparison with data obtained for *Synechocystis* assays in the absence and presence of ethanol. For simplicity, only results with the WT are shown, although UL 004 and UL 030 showed similar results.

Synechocystis WT exponentially growing and dead (resuspended in ethanol 75% v/v for 5 min) cells were stained with CFDA and PI (Fig. 2a)–d)). The ethanol-treated cells were not stained with CFDA, as most of the cells remained in the bottom left quadrant (99.82%) (Fig. 2b), but were stained with PI, as most of the cells moved to the upper left quadrant (99.54%) (Fig. 2d) and the opposite was verified with live cells (Fig. 2a) and c)).

Flow cytometry was also used to monitor the impact of ethanol on WT, UL 004 and UL 030 morphology. It has been reported that microalgae can be detected from the background, based on their intrinsic light scattering properties in forward angle light scatter (FSC) and right angle light scatter (SSC) [31,32]. FSC is measured in the plane of the laser beam and gives information on cell size, while SSC is measured at 90° to the beam detecting different cross sectional areas, thus providing information on the internal structure of the cell or cell granularity, such as cytoplasmic granules, vacuoles and organelles. Aggregates can also be observed in the FSC/SSC plot, as larger and complex events [11]. Fig. 2e) and f) show FSC and SSC signals of ethanol non-treated and treated WT cells, respectively. In both cases, WT cells were observed as homogeneous and elliptical populations in the middle of the plot, indicating that no cell aggregation occurred. Debris was also depicted in the bottom left corner. While the cyanobacteria FSC signals decreased after the ethanol treatment (average FSC = 91 and 53, before and after the ethanol treatment, respectively) the SSC signals increased (average SSC = 184 and 218, before and after the ethanol treatment respectively) (Fig. 2e) and f)) indicating that the cell size decreased and the internal complexity increased, because of the alcohol treatment. Ethanol, being a lipophilic

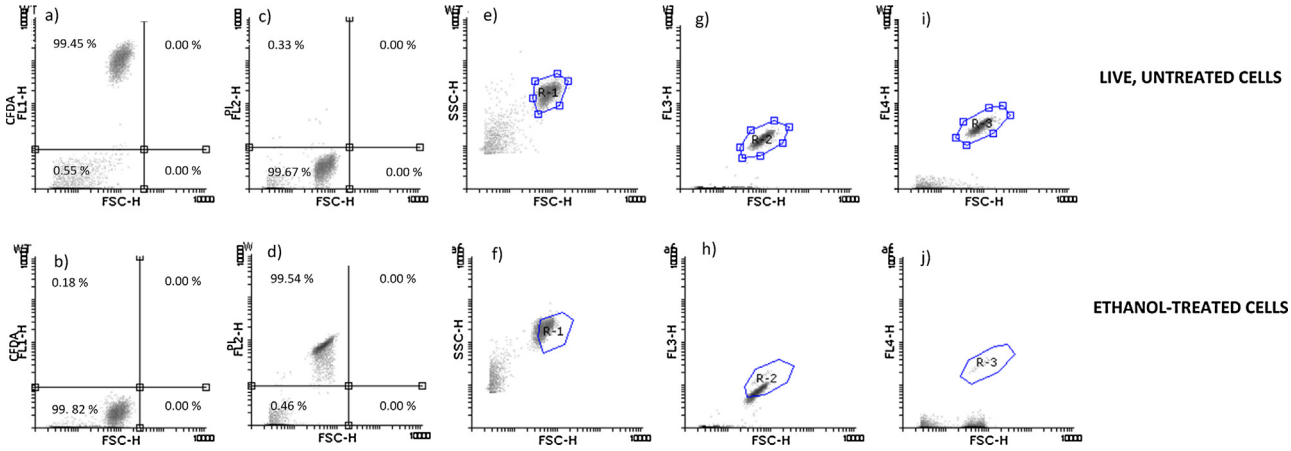

Fig. 2. Flow cytometric controls – WT Density plots concerning CFDA staining (a, b), PI staining (c, d), FSC/SSC signals (e, f), autofluorescence FL3 signal, detecting Chorophyll signal (g, h), autofluorescence FL4 signal, detecting phycocyanin signal (i, j).
a), c), e), g), i) – Cells collected from a WT exponential growing culture
b), d), f), h), j) – WT dead cells treated with ethanol 70% (5 min incubation)
The percentages of cells in each quadrant, calculated by the Flowing Software, are displayed in the density plots a), b), c) and d).
PCEA correspond to the proportion of cells stained with CFDA, thus with enzymatic activity; therefore it is read in the upper left quadrant of the plots FL1 versus FSC-H (Fig. 2a) and b)).
PCIM correspond to the proportion of cells not stained with PI, thus with intact membrane; therefore it is read in the bottom left quadrant of the plots FL2 versus FSC-H (Fig. 2c) and d)).

molecule, dissolves in the cytoplasmic membrane, destroying the phospholipid chains. This may result in cellular content leakage because of the membrane destruction. As cells lost their internal content they shrunk, which may explain the FSC signals decrease and SSC increase.

In addition, microalgal autofluorescence allows microalgal particle discrimination in flow cytometric analysis [32]. Beyond chlorophyll (that is excited at 488 nm and emits fluorescence at wavelengths >670 nm) cyanobacteria produce other fluorescent pigments such as C-phycocyanin, which is the dominant pigment in blue-green algae, and is excited at 640 nm emitting fluorescence at 650 nm. These pigments can be detected by flow cytometry, at the FL3 detector (670 LP) and FL4 detector (675 ± 12.5) respectively. Indeed, chlorophylls and phycocyanin have been used to discriminate cyanobacteria from other particles and microalgae species [33]. Fig. 2g) and i) show the density plots concerning the cell autofluorescence detected in the FL3 (chlorophyll) and FL4 (phycocyanin) detectors of WT non-treated cells. Well defined and homogeneous populations were observed in both plots, inside R2 and R3 regions. As expected, FL3/FSC and FL4/FSC plots (Fig. 2g) and i)) showed a better differentiation of the cyanobacteria population (R2 and R3 regions) from the background than R1 region displayed in the FSC/SSC plot (Fig. 2e)), due to the fact that the R2 and R3 populations are composed of cells containing pigments that emit fluorescence detected in FL3 and FL4 detectors, while the FSC/SSC plot depicts all the events (algae and non-algae particles) that cross the laser beam, thus not differentiating microalgae from other particles.

Figs. 2j) and 2h) show WT ethanol-treated cells (70% (v/v) for 5 min) FL3 and FL4 fluorescence, respectively. The population gated in R2 region (Fig. 2g)) decreased the FL3 signal (Fig. 2h)) after the ethanol treatment (FL3 = 14.40 and 6.73, before and after the ethanol treatment, respectively), indicating that the chlorophyll content decreased after the ethanol treatment, possible because ethanol dissolves this pigment. The population inside R2 region that emitted fluorescence at the FL3 channel was maintained after the treatment (Fig. 2h)).

The effect of the ethanol on WT phycocyanin content is depicted in Figs. 2j) and 2i). After the ethanol treatment, most events in R3 region disappeared (Fig. 2j)). This is not entirely surprising, since phycocyanin is a pigment-protein complex that is denatured by ethanol. These results demonstrated that, when studying the effect of ethanol on cyanobacteria, the flow cytometric discrimination of particles that emit fluorescence in the FL3 channel (which are algae due to the chlorophyll presence) ensures the differentiation of microalgae from other particles and microorganisms, while particles that emit fluorescence in the FL4 detector (due to phycocyanin) cannot be used as a discriminator because the alcohol denatured them.

These preliminary control experiments demonstrated that the CFDA stain in association with flow cytometry can differentiate cells with enzymatic activity, from those that have their enzymatic system affected. PI also allowed distinguishing cells with an intact membrane from those with a permeabilized membrane and FSC and SSC signals can give information on the cyanobacteria morphology, which changed by the effect of ethanol. During the assays with ethanol, gating on FL3 cyanobacteria population ensured that non-algal particles were excluded from the flow cytometric analysis.

3.2. Growth

Table 2 shows the kinetic parameters for all the experiments carried out in the range of 0–40 g/l of added ethanol. However, in Fig. 3, only the growth curves for the assays performed in the absence of ethanol and in the presence of 15, 20 and 30 g/l ethanol are shown, to allow more clarity in analyzing the results obtained, as the profiles for 1, 5 and 10 g/l assays were similar to the one of 15 g/l for all the strains tested. Additionally, as can also be observed in Table 2, no significant differences among the results for cultures at 1, 5 and 10 g/l of ethanol are observed, while growth at 15, 20 and 30 g/l was severely affected to different extent for each strain. The experiments were run around 25–30 days until reaching the stationary phase and, by then, the ethanol remaining in the flasks was about 40% of the initial amounted added, in all cases. Nevertheless, the results obtained for all the three strains were comparable for each concentration level as ethanol evaporation was similar in *Synechocystis* WT, UL 004 and UL 030 growth runs, as well as in blank experiments (without microbial inoculation) performed at the same time.

Table 2
Kinetic data for *Synechocystis* strains WT, UL 004 and UL 030, grown in the presence of different initial ethanol concentrations.

	WT				UL 004				UL 030			
Initial Ethanol concentration (g/L)	X_{max} [a] g/L	X_{maxi}/X_{max0}	μ_{max} [b]/h	μ_{maxi}/μ_{max0}	X_{max} g/L	X_{maxi}/X_{max0}	μ_{max}/h	μ_{maxi}/μ_{max0}	X_{max} g/L	X_{maxi}/X_{max0}	μ_{max}/h	μ_{maxi}/μ_{max0}
0	1.88 ± 0.22	1.00	0.0167 ± 0.0012	1.00	1.78 ± 0.32	1.00	0.0169 ± 0.0011	1.00	1.96 ± 0.15	1.00	0.0190 ± 0.0003	1.00
1	2.35 ± 0.00	1.25	0.0167 ± 0.0005	1.00	1.80 ± 0.07	1.01	0.0159 ± 0.0004	0.94	1.99 ± 0.29	1.02	0.0178 ± 0.0005	0.94
5	2.47 ± 0.20	1.31	0.0164 ± 0.0007	0.98	1.63 ± 0.42	0.92	0.0149 ± 0.0001	0.88	1.78 ± 0.01	0.91	0.0185 ± 0.0007	0.97
10	1.40 ± 0.05	0.74	0.0185 ± 0.0007	0.97	1.42 ± 0.03	0.80	0.0164 ± 0.0009	0.97	2.19 ± 0.28	1.12	0.0179 ± 0.0006	0.94
15	1.06 ± 0.07	0.56	0.0131 ± 0.0000	0.78	1.33 ± 0.38	0.75	0.0159 ± 0.0016	0.94	1.97 ± 0.12	1.00	0.0152 ± 0.0001	0.80
20	0.76 ± 0.11	0.40	0.0090 ± 0.0023	0.54	0.69 ± 0.06	0.39	0.0058 ± 0.0004	0.35	1.55 ± 0.29	0.79	0.0079 ± 0.0000	0.41
30	0.09 ± 0.05	0.05	–		0.07 ± 0.00	0.04	–		0.03 ± 0.01	0.01	–	
40	0.03 ± 0.01	0.02	–		0.05 ± 0.01	0.03	–		0.02 ± 0.00	0.01	–	

[a] Xmax values correspond to data of the first point of stationary phase (usually the highest value of biomass concentration).
[b] μmax values were calculated from the logarithmic plot of the OD readings values in the initial exponential phase.

For all the assays, after a logarithmic phase of about 100 h, the cyanobacterial growth slowed down for a long period, until reaching the stationary phase after more than 500 h (Fig. 3a)–c)), suggesting that, during that period (100 h < t < 500 h) the cultures were limited by a nutrient or conditions such as carbon dioxide availability and/or light.

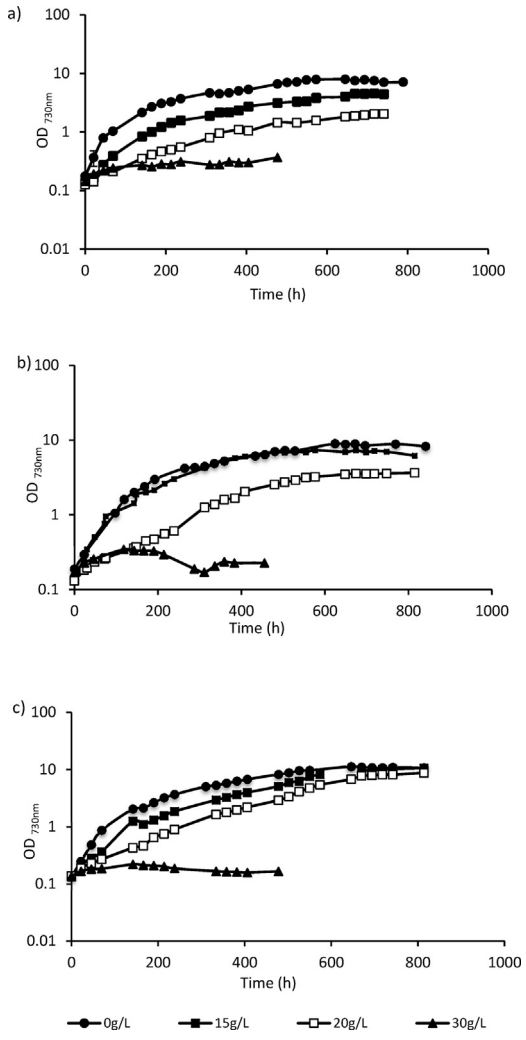

Fig. 3. Evolution of optical density readings at 730 nm during WT (a), UL 004 (b) and UL 030 (c) batch cultures, in the presence of increasing initial ethanol concentrations. OD_{730} averages resulted from two independent replicates (n = 2) and were affected by a relative error not exceeding 15%.

In all cases, at 30 g/l and 40 g/l of ethanol, the cyanobacterial growth was inhibited (Table 2, Fig. 3), seeming that an ethanol concentration of 30 g/l is probably the upper limit of the resistance of all the *Synechocystis* strains.

The ratio maximum biomass concentration/maximum biomass concentration observed for the control assay (X_{max}/X_{max0}) and the ratio maximum specific growth rate/maximum specific growth rate observed for the control assay ratio (μ_{max}/μ_{max0}) were calculated as a measure of the impact of the ethanol on X_{max} relatively to X_{max0} (Table 2). For lower initial ethanol concentrations (<5 g/l), X_{max} values were similar for all the strains. However, X_{max}/X_{max0} ratios around 0.75 were observed for the three strains at initial ethanol concentrations progressively higher (10 g/l for WT; 15 g/l for UL 004; and 20 g/l for UL 030), indicating that the UL 030 strain was the most tolerant to the alcohol. Above 30 g/l of ethanol, X_{max} values were below 0.1 g/l, confirming that, for all the strains, growth was inhibited at these ethanol initial concentrations.

The specific growth rate decreased, as expected, as the initial ethanol concentration increased (Table 2). The highest μ_{max} values were observed for UL 030 strain for initial ethanol concentrations up to 5 g/l. Nevertheless, μ_{max}/μ_{max0} ratios higher than 0.9 were only observed for UL 004 strain at ethanol initial concentration up to 15 g/l, while WT and UL 030 displayed this μ_{max}/μ_{max0} ratio up to 10 g/l.

3.3. Physiological response

Figs. 4 and 5 show, respectively, the enzymatic activity and membrane integrity for the three *Synechocystis* strains for the control assay (0 g/l of ethanol) and assays carried out at 15, 20 and 30 g/l of ethanol. Fig. 4 displays for strains WT and UL 004 the proportion of cells with enzymatic activity (PCEA) decreasing as the culture aged, particularly after 400 h, when the cultures attained the stationary phase (Fig. 3a) and b)), and this decrease was more pronounced as the ethanol initial concentration increased (Fig. 4a) and b)). This was expected, since cells are more vulnerable during the stationary phase, as they are experiencing starvation and/or adverse environmental conditions, being more vulnerable to the presence of ethanol. Comparing the PCEA profiles for WT and UL 004, at ethanol concentrations in the range of 0–20 g/l, the latter showed higher PCEA (above 80%) until t = 400 h, while the former showed a progressive PCEA decrease after t = 135 h, as the initial ethanol concentrations increased. After 231 h, WT assay at 30 g/l of ethanol displayed a PCEA of 60 %, while at t = 287 h, UL 004 assays at 30 g/l displayed a PCEA of 93% (Fig. 4a) and b)).

UL 030 strain showed a completely different PCEA profile, compared to the remaining strains (Fig. 4c)). UL 030 assays at 0, 15

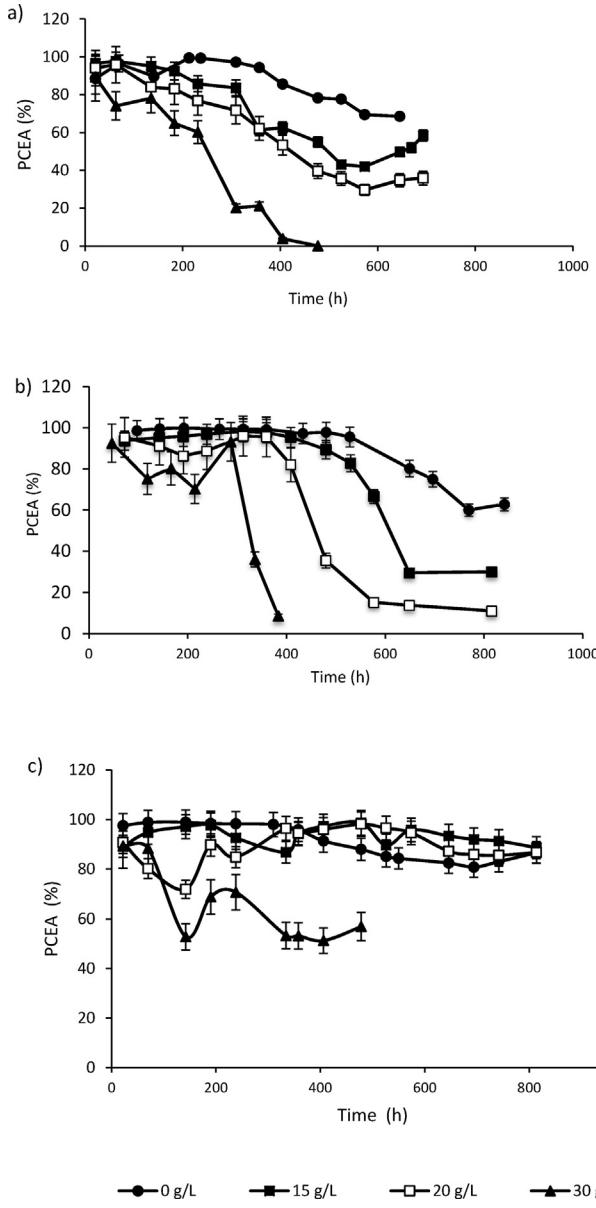

Fig. 4. PCEA evolution during WT (a), UL 004 (b) and UL 030 (c) batch cultures, in the presence of increasing initial ethanol concentrations. Error bars correspond to the standard deviation resulted from two independent replicates (n = 2).

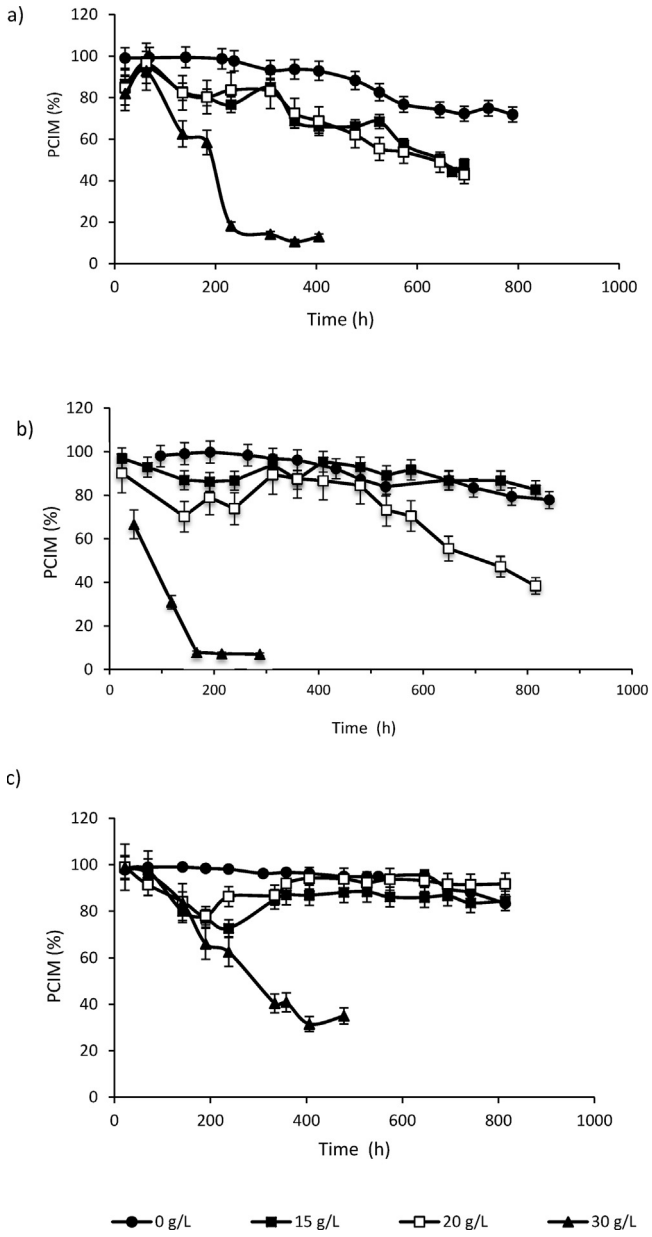

Fig. 5. PCIM changes during WT (a), UL 004 (b) and UL 030 (c) batch cultures, in the presence of increasing initial ethanol concentrations. Error bars correspond to the standard deviation resulted from two independent replicates (n = 2).

and 20 g/l displayed a high PCEA (>80%) throughout the entire cultivation time course, indicating that the UL 030 strain was more resistant to the stationary phase adverse conditions, with its enzymatic system being almost unaffected by the presence of ethanol. In addition, in the assay at 30 g/l of ethanol, after 400 h, the UL 030 showed a higher PCEA than WT and UL 004 ($PCEA_{WT}$ = 0%; $PCEA_{UL004}$ = 7%; $PCEA_{UL030}$ = 53%). The membrane integrity results are shown in Fig. 5a)–c) for assays conducted at 0, 15, 20 and 30 g/l ethanol. WT assays in the range of 0–10 g/l of ethanol showed a proportion of cells with intact membrane (PCIM) between 99% and 68% throughout the cultivation time course (data not shown for clarity of the plot). PCIM of WT assays at 15 g/l and 20 g/l of ethanol decreased abruptly after 309 h, achieving 48% and 42% respectively, at the end of the experiments. In general, WT PCEA values were below WT PCIM values Figs. 4a) and 5a). Also, PCEA values were more severely reduced after 309 h when the PCIM values started decreasing, and this was particularly evident for assays at 15 g/l and 20 g/l of initial ethanol concentration. In fact, beyond the esterase activity inhibition due to the presence of ethanol, changes in the cyanobacteria membrane permeability could have as well contributed for the decrease in the WT cells CFDA fluorescence [12], thus, in the PCEA. For WT assay at 30 g/l, PCIM sharply decreased, attaining 12% at t = 400 h.

UL 004 showed a different PCIM profile when compared to WT PCIM profile (Fig. 5a) and b)). Indeed, for experiments at ethanol initial concentrations in the range of 0–15 g/l, UL 004 PCIM was always above 80% during the cyanobacteria cultivations time course indicating that UL 004 cytoplasmic membrane was more resistant to the ethanol in this ethanol concentrations range than the WT strain, as above referred. Nevertheless, for the assay at 15 g/l, despite UL004 PCIM having been always above 80% throughout the cultivation time course (Fig. 5b)), PCEA was drastically reduced after 359 h (Fig. 4b)), which meant that UL 004 cells still had intact membranes, despite the affected enzymatic system. For the assay at 20 g/l of initial ethanol, both PCEA and PCIM concomitantly

decreased (Figs. 4b)). At t = 648 h, 86% of the cells had intact membrane, but only 30% of the cells displayed enzymatic activity. These results demonstrated that a high proportion of UL 004 cells could maintain their cytoplasmic membrane intact at 15 g/l of ethanol but not at 20 g/l of ethanol. Comparing with WT data, UL 004 was more resistant to the alcohol, since the latter could maintain a high PCIM at 15 g/l, while the former could not. At 20 g/l, both strains showed a significant decrease in both PCEA and PCIM while at 30 g/l and 40 g/l UL 004 PCIM started decreasing from the beginning of the experiment as observed also for the WT strain.

Strain UL 030 PCIM was almost always higher than 80% over the entire cultivation time-course (Fig. 5c)) for the assays at 0–20 g/l of initial ethanol concentration. In this case, both UL 030 PCEA and PCIM remained always high (>80%) during the assay at 20 g/l of ethanol, revealing a significant ethanol resistance improvement when comparing to WT and UL 004 strains. For assay at 30 g/l ethanol, UL 030 PCIM started decreasing since the experiment launch as observed for the remaining strains.

Previous work [9] reported that UL030 strain ethanol productivity was 57% higher than the single cassette strain UL004 (0.285 g/l d and 0.181 g/l d respectively) when both strains were cultivated in BG-11 media, under similar growth and light conditions in shake flasks. This result, together with the flow cytometric results above described, suggest that the most efficient ethanol producer (strain UL 030) was the most tolerant to ethanol. The explanation for the higher UL 030 ethanol tolerance may be due to the fact that higher levels of ethanol produced by UL 030 probably induces an adaptive response, becoming more tolerant as the levels of ethanol increase, which is in accordance with previous published studies. Qiao et al. [11] added 1.5% ethanol and examined the proteomic response. 32 unique proteins were up-regulated while some 42 were down-regulated after 24 h. Many were involved in the common stress response indicating that the organism was adapting to the ethanol. Borirak et al. [34] analyzed the proteomic response of ethanol production by an engineered *Synechocystis* strain rather in response to added ethanol in an engineered strain SAA012 similar to UL 040 with a single ethanol cassette. Here the proteomic response was less than that observed for added ethanol as would be expected as the level of ethanol was lower some 9.88 mM over the 19 days of analysis. However a number of proteins including those involved in oxidative stress were up-regulated suggesting that the organism was adapting to the ethanol and responding. Transcriptomic analysis of *Synechocystis* in response to added ethanol revealed some 274 genes up-regulated with the response [35] being broadly similar to that reported by Qiao et al. [11]. Dienst et al. [36] analyzed the transcriptome with continuous metabolic engineered production in strains similar to UL 004 and found that the response was less than that observed by Nie et al. [35] but broadly in line with the proteome study of Borirak et al. [34]. Thus it appears that *Synechocystis* is responding differentially to different levels of ethanol. Presumably, at low levels of ethanol, the organism is adapting and becoming tolerant by a low level response while as the level of ethanol increases the response is increasing. Thus it is expected that the increased levels of ethanol produced by UL 030 relative to UL 004 is eliciting a stronger response such that the organism is adapting and, presumably, becoming more tolerant as the levels of productivity increase, in line with the transcriptomic and proteomic studies reported [11,34–36].

3.4. Morphological changes

For all the strains, at ethanol concentrations higher than 15 g/l, cell aggregation was observed, and the aggregates increased in size and density, as the culture aged and the initial concentration of added ethanol increased.

Fig. 6 shows the density plots SSC/FSC and the optical microscope observations for the three strains in the absence and presence of 30 g/l and 40 g/l of ethanol, before sedimentation, at t = 70 h. For the control assay of all the strains, an elliptical and homogeneous population can be seen in the SSC/FSC plots (Fig. 6a), g) and m)), indicating that no cell aggregation occurred. Indeed, the microscopy observations (Fig. 6d), j) p)) showed individual cells. At 30 g/l of ethanol, WT and UL 004 cells formed aggregates, as shown in the density plots (Fig. 6b) and h)) displaying a broad, oblique and heterogeneous distribution, because of the different sizes of the events that crossed the laser beam. In fact, the optical observations showed the presence of aggregates (Fig. 6e) and k)). UL 030 cells aggregated in a less extension when comparing to the other strains, as confirmed in the FSC/SSC plots (Fig. 6n) and o)) and microscope observations (Fig. 6q) and r)). Qiao et al. [11] also reported cell aggregation after 24 h when *Synechocystis* sp. PCC 6803 was grown in the presence of 15 g/l ethanol as a stress response to the alcohol presence. Anfelt et al. [37] studied *Synechocystis* sp. PCC 6803 transcriptomic stress response to the butanol presence, and suggested that *pilA1 (sll1694)* and *pilA4 (slr1456)* proteins, part of the upregulated two-component-system genes that encoded pilus assembly proteins, could possibly play a role in the cell aggregation observed in cultures containing high butanol concentrations. On the other hand, it has been proposed that extracellular polymeric substances, mainly of polysaccharidic nature (exopolysaccharides (EPS)) are involved in *Synechocystis* cell aggregation mechanism, operating in the cell protection against environmental stresses [38]. Jittawuttipoka et al. [39] demonstrated that EPS protect *Synechocystis* PCC6803 cells from salt and heavy metal stresses, and suggested that EPS, in surrounding cells, behave as a physico-chemical barrier preventing direct contact between cells and toxics or adverse conditions. These authors also found that EPS-depleted *Synechocystis* mutant cells (doubly deleted for *sll1581* and *slr1875* genes that are associated to the EPS production) could aggregate and form biofilms faster than the WT strain that produced great amounts of EPS, aggregated less, and was more resistance to salt and heavy metal stresses than the EPS-depleted mutants. These results are consistent with previous EPS studies in many other bacteria including *E. coli*, *P. putida*, *S. haemolyticus*, *S. pneumoniae* [40,41] which identified several EPS that inhibit biofilm formation in acting as surfactants.

In the present work, cell aggregation was observed for WT, UL 004 and UL 030 strains at initial ethanol concentrations higher than 15 g/l, showing WT and UL 004 higher cell aggregation tendency then UL 030, as depicted in Fig. 6. This may be associated to the lower tolerance to the ethanol of WT and UL 004 strains (in terms of biomass production, enzymatic activity, membrane integrity, as shown before) when compared with UL 030 behavior in the presence of the alcohol. Indeed, according to Jittawuttipoka et al. [39], *Synechocystis* cell aggregation is associated to a reduced EPS formation, thus, to a lower resistance to environmental stresses. This suggests that the higher ethanol tolerance of strain UL 030 could be associated with increased EPS production, comparing to the other *Synechocystis* strains that displayed lower ethanol tolerance and a greater tendency to aggregate. This may be supported by the fact that, as the *phaA* and *phaB* genes involved in the poly-b-hydroxybutyrate (PHB) pathway synthesis were deleted in UL 030 strain, carbon might be diverted towards EPS production. At 40 g/l of ethanol cell aggregation was reduced for all the strains (Fig. 6c), f), i), l), o), and r)).

As the cultures aged, the aggregates formed during WT and UL 004 assays at 30 g/l and 40 g/l of initial ethanol became more compact and filamentous. At the initial ethanol concentration of 30 g/l, cells remained green (Fig. 7a) and b)), while at 40 g/l, cells turned bleached white (Fig. 7c). Samples were observed under the

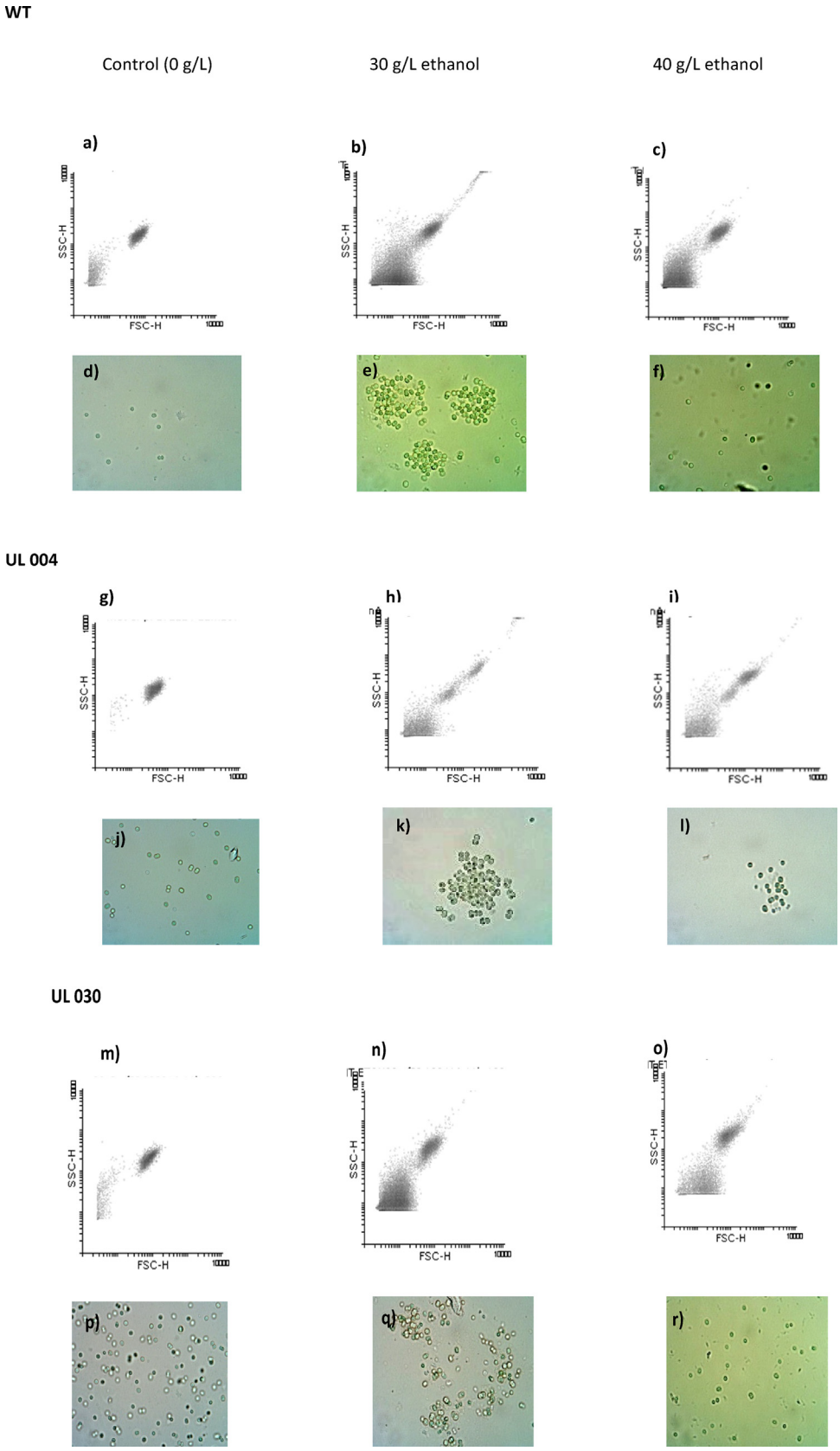

Fig. 6. Density plots SSC/FSC and photos concerning flow cytometric analysis and optical microscope observations of cells collected after 70 h, from WT, UL 004 and UL 030 batch cultures at 0 g/l (control), 30 g/l and 40 g/l of ethanol.
WT SSC/FSC density plots: a)–c)
WT optical microscope photos (1000× magnification): d)–f)
UL 004 SSC/FSC density plots: g)–i)
UL 004 optical microscope photos (1000× magnification): j)–)
UL 030 SSC/FSC density plots: m)–o)
UL 030 optical microscope photos (1000× magnification): p)–r)

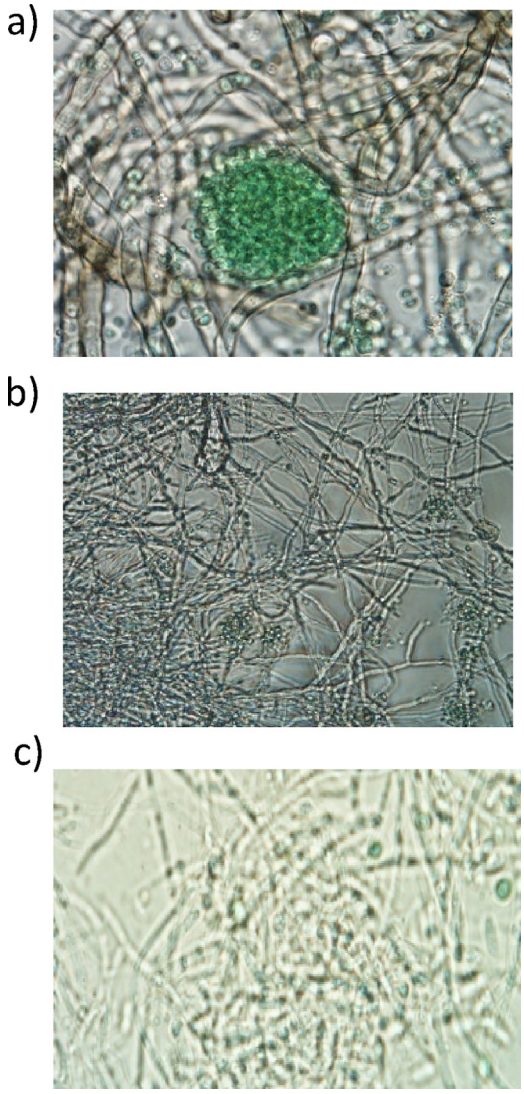

Fig. 7. Optical observations (1000×) of WT (a) and UL 004 (b) cells harvested from batch cultures at initial 30 g/l ethanol and UL 004 (c) cells at 40 g/l ethanol (t = 400 h).

optical microscope, using a blue filter (488 nm), and indeed the chlorophyll pigment was detected confirming that, at these ethanol concentrations, cells could synthesize this pigment, despite the morphological changes. To ensure that these filamentous aggregates were not fungal contaminations, UL 004 strain was grown in the presence of 30 g/l of ethanol and kanamycin. After 400 h, the filamentous forms were observed again. Diluted samples were plated in Rose Bengal medium and no microbial growth was detected nor were *Synechocystis* cells, as chloramphenicol had been added to the Rose Bengal medium. Afterwards, the medium was centrifuged and the pellet was re-inoculated into fresh medium without ethanol, but with kanamycin. After 400 h, the culture was blooming as *Synechocystis* individual cells, as expected. These tests confirmed that the filamentous structures that were observed at higher ethanol concentrations are indeed a stress response of *Synechocystis* to the presence of ethanol. As far as we are aware, there is no description in literature about the capability of *Synechocystis* to form filaments, under stress conditions. Also, the results from these tests reinforce the previous conclusions that the ethanol concentration of 30 g/l is the upper limit of the survival of the *Synechocystis* strains.

Table 3
Physiological and morphological changes for *Synechocystis* WT, UL 004 and UL 030 strains after 400 h in the presence of 30 g/L of ethanol.

Strain	Cells with enzymatic activity (%)	Cells with intact membrane (%)	Morphological changes (Aggregation/Filamentous)
WT	0.0 ± 0.0	13.0 ± 1.3	++/++
UL 004	8.7 ± 0.8	10.2 ± 1.0	++/++
UL 030	51.2 ± 5.1	31.5 ± 3.1	+/−

Table 3 summarizes WT, UL 004 and UL 030 behavior in the presence of 30 g/l initial ethanol, at t = 400 h, wherein major physiological and morphological differences among the strains were observed.

UL 030 depicted the highest ethanol tolerance as compared to the other strains, in terms of PCEA and PCIM, and this was accompanied by morphological changes. The lower aggregation/filamentous formation shown by this strain appeared to be associated with higher ethanol resistance.

4. Conclusions

The results obtained in this work demonstrated that the recombinant *Synechocystis* strains tested (UL 004 and UL 030) were more tolerant to the presence of ethanol than the WT strain, and the most efficient ethanol producer (UL 030) was the most tolerant to ethanol. Flow cytometry was successful in evaluating the ethanol tolerance response of *Synechocystis* strains, in terms of enzymatic activity, membrane integrity and morphological changes.

To efficiently utilize any of these metabolic engineered recombinants for industrial bioethanol production, the process should be conducted at bulk ethanol concentrations below 15 g/l, to ensure that the cyanobacteria cells stay metabolically active and productive.

Conflict of interest

None.

Acknowledgements

This work was carried out within the FP7 DEMA “Direct Ethanol from Microalgae” project, which received funding from the European Union’s Seventh Framework Programme for Research, Technological Development and Demonstration under grant agreement no 309086. The authors also acknowledge Graça Gomes (UB/LNEG), Natércia Santos (UB/LNEG) and Margarida Monteiro (UB/LNEG) for microalgae culture maintenance and laboratorial support. The author has confirmed that the Acknowledgment text is according to the 7 model grant agreement rules.

References

[1] S.P. Cuellar-Bermudez, J.S. Garcia-Perez, B.E. Rittmann, Photosynthetic bioenergy utilizing CO2: an approach on flue gases utilization for third generation biofuels, J. Clean. Prod. 98 (2015) 53–65.
[2] C. Charles, Should we be concerned about competition between food and fuel? Analysis of biofuel consumption mandates in the European Union and the United States, International Institute for SustainableDevelopment, 2012.
[3] C. Weber, A. Farwick, F. Benish, E. Boles, Trends and challenges in the microbial production of lignocellulosic bioalcohol fuel, Appl. Microbiol. Biotechnol. 87 (2010) 1303–1315.
[4] Z. Gao, H. Zhao, Z. Li, X. Tan, X. Lu, Photosynthetic production of ethanol from carbon dioxide in genetically engineered cyanobacteria, Energy Environ. Sci. 5 (2012) 9857–9865.
[5] J. Dexter, P.C. Fu, Metabolic engineering of cyanobacteria for ethanol production, Energy Environ. Sci. 2 (2009) 857–864.

[6] J. Dexter, P. Armshaw, C. Sheahan, J.T. Pembroke, The state of autotrophic ethanol production in cyanobacteria, J. Appl. Microbiol. 119 (2015) 11–24.
[7] M.-D. Deng, J.R. Coleman, Ethanol synthesis by genetic engineering in cyanobacteria, Appl. Environ. Microbiol. 65 (1999) 523–528.
[8] N.-S. Lau, M. Matsui, A.A. Abdullah, Cyanobacteria photoautotrophic microbial factories for the sustainable synthesis of industrial products, Biomed. Res. Int. (2015)754934.
[9] P. Armshaw, D. Carey, L. Quinn, C. Sheahan, J.T. Pembroke, Optimization of ethanol production in *Synechocystis* PCC 6803, the DEMA approach, Solar Fuels Conference, Uppsala, Sweden, 2015 (Available in: http://www.dema-etoh.eu/admin/common/files/1459503476_dema-poster-solar-apr-2015-v2.pdf).
[10] J. Kämäräinen, H. Knoop, N.J. Stanford, F. Guerrero, M.K. Akhtar, E.M. Aro, R. Steuer, P.R. Jones, Physiological tolerance and stoichiometric potential of cyanobacteria for hydrocarbon fuel production, J. Biotechnol. 30 (2012) 67–74.
[11] J. Qiao, J. Wang, L.X. ChenTian, S. Huang, X. Ren, W. Zhang, Quantitative iTRAC LC-MS/MS proteomics reveals metabolic responses to biofuels ethanol in cyanobacterial *Synechocystis* sp. PCC6803, J. Proteome Res. 11 (2012) 5286–5300.
[12] N.M. Franklin, M.S. Adams, J.L. Stauber, R.P. Lim, Development of an improved rapid enzyme inhibition bioassay with marine and freshwater microalgae using flow cytometry, Arch. Environ. Contam. Toxicol. 40 (2001) 469–480.
[13] J.L. Stauber, N.M. Franklin, M.S. Adams, Applications of flow cytometry to ecotoxicity testing using microalgae, Trends Biotechnol. 20 (2002) 141–143.
[14] X. Xi, H. Zhi-ying, C. Ying-xu, K. Xin-qiang, L. Hua, Q. Yi-chao, Optimizing of FDA-PI method using flow cytometry to measure metabolic activity of the cyanobacteria, *Microcystis aeruginosa*, Phys. Chem. Earth 36 (2011) 424–429.
[15] J.R. Gumbo, Y.E. Cloete, G.J.J. van Zyl, J.E.M. Sommerville, The viability assessment of *Mycrocystis aeruginosa* cells after co-culturing with Bacillus mycoides B16 using flow cytometry, Phys. Chem. Earth 72–75 (2014) 24–33.
[16] D. Latour, O. Sabido, M.J. Salençon, H. Giraudet, Dynamics and metabolic activity of the benthic cyanobacterium *Microcystis aeruginosa* in the Grangent reservoir (France), J. Plankton Res. 26 (2014) 719–726.
[17] M.G. Silveira, M.V. Romão, M.C. Loureiro-Dias, F. Rombouts, T. Abee, Flow cytometric assessment of membrane integrity of ethanol-stressed *Oenococcus oeni* cells, Appl. Environ. Microbiol. 69 (2002) 6087–6093.
[18] S.C. Albers, C.A.M. Peebles, Evaluating light-induced promoters for the control of heterologous gene expression in *Synechocystis* sp. PCC 6803, Biotechnol. Prog. 33 (2016) 45–53.
[19] R. Vidal, L. López-Maury, M.G. Guerrero, F.J. Florencio, Characterization of an alcohol dehydrogenase from the cyanobacterium *Synechocystis* sp. strain PCC 6803 that responds to environmental stress conditions via the hik34-Rre1 two-component system, J. Bacteriol. 191 (2009) 4383–4391.
[20] D. Böltner, C. MacMahon, J.T. Pembroke, P. Strike, A.M. Osborn, R391 is an 89 kb conjugative genomic island comprising elements related to plasmids phages, and transposable elements, J. Bacteriol. 184 (2002) 5158–5169.
[21] F. Pinto, C.C. Pacheco, P. Oliveira, A. Montagud, A. Landels, N. Couto, P.C. Wright, J.F. Urchueguía, P. Tamagnini, Improving a *Synechocystis*-based photoautotrophic chassis through systematic genome mapping and validation of neutral sites, DNA Res. 22 (2015) 425–437.
[22] T.F. Knight, R.P. Shetty, D. Endy, Engineering BioBrick vectors from BioBrick parts, J. Biol. Eng. 2 (2008) 1–12, doi:http://dx.doi.org/10.1186/1754-1611-2-5.
[23] P. Armshaw, D. Carey, C. Sheahan, J.T. Pembroke, Utilizing the native plasmid, pCA2.4 from the cyanobacterium *Synechocystis* sp. strain PCC 6803 as a cloning site for enhanced product production, Biotechnol. Biofuels 8 (2015) 201.
[24] J. Norrander, T. Kempe, J. Messing, Construction of improved M13 vectors using oligodeoxynucleotide-directed mutagenesis, Gene 26 (1983) 101–106.
[25] X. Zang, B. Liu, S. Liu, K. Arunakumara, X. Zhang, Optimum conditions for transformation of *Synechocystis* sp. PCC 6803, J. Microbiol.-Seoul 45 (2007) 241–245.
[26] J. Wang, L. Chen, S. Huang, J. Liu, X. Ren, X. Tian, J. Qiao, W. Zhang, RNA-seq based identification and mutant validation of gene targets related to ethanol resistance in cyanobacterial *Synechocystis* sp. PCC 6803, Biotechnol. Biofuels 5 (2012) 89.
[27] Z. Song, L. Chen, J. Wang, Y. Lu, W. Jiang, W. Zhang, A transcriptional regulator sll0794 regulates tolerance to biofuel ethanol in photosynthetic *Synechocystis* sp. PCC 6803, Mol. Cell. Proteomics 13 (2014) 3519–3532.
[28] Y. Zhang, X. Niu, M. Shi, G. Pei, X. Zhang, L. Chen, W. Zhang, Identification of a transporter Slr0982 involved in ethanol tolerance in cyanobacterium *Synechocystis* sp. PCC 6803, Front. Microbiol. 6 (2015) 487.
[29] Y. Zhu, G. Pei, X. Nei, M. Shi, M. Zhang, L. Chen, W. Zhang, Metabolomic analysis reveals functional overlapping of three signal transduction proteins in regulating ethanol tolerance in cyanobacterium *Synechocystis* sp. PCC 6803, Mol. Biosyst. 11 (2015) 779–782.
[30] R. Vidal, Alcohol dehydrogenase AdhA plays a role in ethanol tolerance in ethanol tolerance in model cyanobacterium *Synechocystis* sp. PCC 6803, Appl. Microbiol. Biotechnol. 101 (2017) 3473–3482.
[31] T. Lopes da Silva, A. Reis, The use of multi-parameter flow cytometry to study the impact of n-dodecane additions to marine dinoflagellate microalga *Crypthecodinium cohnii* batch fermentations and DHA production, Ind. Microbiol. Biotechnol. 35 (2008) 875–887.
[32] P. Hyka, S. Lickova, P. Přibyla, K. Melzochb, K. Kovara, Flow cytometry for the development of biotechnological processes with microalgae, Biotechnol. Adv. 31 (2013) 2–16.
[33] A. Becker, A. Meister, C. Wilhelm, Flow cytometric discrimination of various phycobilin-containing phytoplankton groups in a hypertrophic reservoir, Cytometry 48 (2002) 45–57.
[34] L. Borirak, A. Koning, H. Woude, H. Hoefsloot, W. Dekker, C. Roseboom, K. Koster, Quantitative proteomics analysis of an ethanol- and a lactate-producing mutant strain of *Synechocystis* sp. PCC 6803, Biotechnol. Biofuels 8 (2015) 111.
[35] L. Nie, G. Wu, D.E. Culley, J.C. Scholten, W. Zhang, Integrative analysis of transcriptomic and proteomic data: challenges, solutions and applications, Crit. Rev. Biotechnol. 27 (2007) 63–75 (D).
[36] J. Dienst, T. Georg, L. Abts, E. Jakorew, A. Bömer, U. Wilde, H. Dühring, W.R. Enke, Transcriptomic response to prolonged ethanol production in the cyanobacterium *Synechocystis* sp. PCC 6803, Biotechnol, Biofuels 7 (2014) 21.
[37] J. Anfelt, B. Hallström, J. Nielsen, M. Uhlén, E.P. Hudson, Using transcriptomics to improve butanol tolerance of *Synechocystis* sp. strain PCC 6803, Appl. Environ. Microbiol. 79 (2013) 7419–7427.
[38] R. De Philippis, G. Colica, E. Micheletti, Exopolysaccharide-producing cyanobacteria in heavy metal removal from water: molecular basis and practical applicability of the biosorption process, Appl. Microbiol. Biotechnol. 92 (2011) 697–708.
[39] T. Jittawuttipoka, M. Planchon, O. Spalla, K. Benzerara, F. Guyot, C. Cassier-Chauvat, F. Chauvat, Multidisciplinary evidences that *Synechocystis* PCC 6803 exopolysaccharides operate in cell sedimentation and protection against salt and metal stresses, Plus One 8 (2013) e55564.
[40] M. Nilsson, W.C. Chiang, M. Fazli, M. Gjermansen, M. Givskov, T. Tolker-Nielsen, Influence of putative exopolysaccharide genes on *Pseudomonas putida* KT2440 biofilm stability, Environ. Microbiol. 13 (2012) 1357–1369.
[41] O. Rendueles, J.B. Kaplan, J.M. Ghigo, Antibiofilm polysaccharides, Environ. Microbiol. 15 (2012) 334–346.